© 2017 IJSRST | Volume 3 | Issue 8 | Print ISSN: 2395-6011 | Online ISSN: 2395-602X
Themed Section: Science and Technology

Simulation of Residual Stresses in Castings

B. Venu[1], Dr. R. Ramachandra[2]

[1]M.Tech Student, Dept. of Mechanical Engineering, SKD Engineering College, Gooty, Anantapur, Andhra Pradesh, India
[2]Principal & Professor, Dept. of Mechanical Engineering, SKD Engineering College, Gooty, Anantapur, Andhra Pradesh, India

ABSTRACT

Unpredictable residual stresses are in most components considered to be a defect. The stresses are formed during the cooling process, caused by the temperature and visco plastic strains. Performing a heat treatment (HT), the material starts to creep and residual stresses can be reduced with over 90% of the total initial stress. This study has been done in order to examine residual stress relieving in the HT for three cast iron materials, VIG-275/190, GJL-250 and GJS-500-7. The purpose is to find the effect of varying parameters and compare the result against simulation. A stress lattice component, designed to create residual stress are used to investigate the stress relieving. Through a sectioning method the stress is released and can be measured by strain gauges placed on the surface. The stresses are measured on each material both as cast and after HT and trough empirical testing the effect of different parameters during the HT was established. Comparing the practical test against simulations by Magma5 the cooling rate during solidification process is too quick in simulations. This fault is attributed to the non-included latent heat release during phase transformation at 723 °C (austenite to pearlite). By changing the specific heat capacity of sand and the cast iron this error can be corrected. The simulations also predict the stress to be fully relieved when reaching the hold temperature of 610 °C, this have been confirmed to be wrong shown by the significant effect of hold time in all investigated materials. The effects of varying cooling rates and drop temperatures are also difficult for the simulations to predict. Heat treatment experiments on of VIG-275/190 shows that the alloying of Molybdenum and Chromium makes the material more resistant against creep at elevated temperatures. The hold time and time spent over 500 °C are the most significant parameters. The unalloyed GJL-250 creeps more easily which makes all the heat treatment parameters more important, i.e. heating rate, hold time and cooling rates. Lastly the ductile iron GJS-500-7 has the highest residual stress in as cast condition and shows the largest stress relief after the heat treatments.

Keywords : Heat Treatment, X-Direction, Solidification, GJL, GJS

I. INTRODUCTION

When the melted metal in a casting process cools down and solidifies, residual stresses arise from the strain caused by viscoplastic flow and temperature gradients. This is because the thermal energy dissipates faster in the thinner sections compared to the thicker sections and causes a temperature gradient in the material leading to residual stresses. While the thinner part is contracting due to the thermal contraction the core is still hot and maintains its larger volume. When the material is further cooled to room temperature the differences in thermal contractions cause residual stresses. In order to get rid of these stresses heat treatment is required. Residual stresses have a significant effect on the materials mechanical properties and the overall performance. High residual stresses can lead to early fatigue, increased crack propagation and potentially fracture the component.

After the solidification process, cast iron components are heat treated to reduce the residual stresses. This will improve the mechanical properties and avoid undesired stress concentrations in the material. As an example a cylinder head has a complex geometry and residual stresses are unwanted and difficult to predict. The assumption is that these stresses can be counteracted and lowered to insignificant levels with a heat treatment. By investigating varying heat treatment parameters and relate them to the relieving of residual stresses a process optimization can be done. This could in turn lead to higher quality components and improve the overall manufacturing process.

The materials that will be investigated are shown below, specific material properties are shown in chapter Investigated materials.

- ✓ Grey iron, GJL-250
- ✓ Grey iron, VIG 275/190 Ductile iron EN-GJS-500-7

The software Magma5 simulates solidification and heat treatment to predict the residual stresses. Simulations save both time and money but have requirements on accuracy and precision to be reliable. Finding discrepancies between practical tests and simulations would bring new aspects to improve the simulations and make them more efficient and precise.

SOLIDIFICATION

The phenomena of melting and solidification has many current engineering applications such as ice formation, solidification of castings and scrap melting in the metal industry, the cooling, freezing and cold storage of foodstuffs in the food industry and certain other problems in chemical engineering (Mastanaiah, 1976).

Among them casting industry is one of the oldest industries in human society and until recently, it was considered to be an art rather than a science. Only after the Second World War, the basic variables in the process of casting industry have been studied in details to have a greater understanding of the interrelations of the factors involved in making a good casting. The foundry technology is fast becoming an applied science with much of mathematical formulae. But still the subject is not yet a complete science because of the number of variable factors involved. With the help of computers, now we are in a better position to tackle metal casting from a scientific point of view.

There are number of casting processes available depending upon the nature of the product. It involves considerable metallurgical and mechanical aspects. Properly designed dies and a good control over the process parameters are considered a must for quality castings. To arrive at the optimum process parameters, the experimental methods are always better than simulations. But from realistic considerations, it is costly and time consuming and many are impossible in some cases. Hence computer simulation of the whole process is a convenient way to design a mould and analyze the effects of various parameters.

METAL CASTING

It is a phase transformation process of liquid to solid state. A metal in molten condition possesses high energy. As the melt cools, it looses energy to form crystals. The crystal growth proceeds with release of energy at the crystal melt interface. Solidification process exerts a very strong influence upon the three properties of cast metal viz.

During solidification, cast form develops cohesion and acquires structural characteristics. Also during solidification, casting acquires the metallographic structures viz. grain size, shape and its orientation, distribution of alloying elements and under lying crystal structures and its imperfections.

The rate of cooling governs the microstructure of casting to a large extent and intern it controls mechanical properties like strength, hardness, machinanability, etc. The magnitude of residual stresses built-up in the casting depends on the geometry of the casting, mould design and thermo mechanical properties of both the cast and the mould process parameters.

In case of very high residual stress accumulation, the casting may develop cracks at the time of processing itself. Low residual stresses may not be high enough to cause cracks during processing but sufficiently high enough to reduce the fatigue life leading to early failure in service.

II. EXPERIMENTAL WORK AND MATERIALS

This chapter describes the practical testing as well as the simulations and how the two parts are performed. Each step of both the practical and simulation experiments is done on all investigated materials, with the exception of simulations of GJL-250.

III. MEASURE RESIDUAL STRESSES WITH SECTIONING METHOD

The elongation (length difference in %) is measured using a strain gauge. Using only one gauge is not sufficient; several gauges are required in order to accumulate accurate data. The strain gauge is a simple

technological tool and yet precise and accurate when measuring resistance.

To measure elongation the strain gauge is fixated into the test pieces surface with a suitable adhesive. The adhesive must cover all of the thin copper wiring to ensure that errors are kept small. The setup of the gauge is simple and uses a Wheatstone bridge to calculate the resistance in the strain gauge. The Wheatstone bridge is the electrical circuit shown in Figure 3.7. Rgauge has an unknown resistivity and can be calculated by knowing all the other resistances. The unknown resistivity changes depending on strain of the section and can thus be used as a way to measure the strain. Figure 3.7 describes the Wheatstone bridge and shows how the gauge is included.

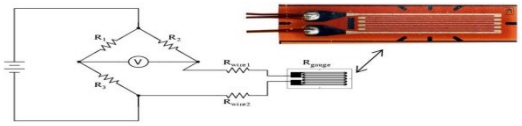

Figure 1. The Wheatstone bridge to measure resistance in a strain gauge

The Rgauge is what is known as the foil in the strain gauge and does a zigzag thread resemble a spring. This is to ensure that the elongation is completely elastic and makes sure that only linear elongation occurs, a necessity for precise results. The resistance is very sensitive to changes. Under tension the area of the thread becomes smaller and resistance increases. Under compressive stress the area grows larger and resistance is lowered. From this the load case and stresses can easily be determined using the equations below. From equations Eq.1 and Eq.1 below, GF is Gauge Factor, ΔR is the change of resistance, Rg is resistance before deforming and BV is the bridge excitation voltage.

Equation 1 and equation 2. The relation used to calculate strain from measured resistance

$$GF = \frac{\Delta R / R_G}{\varepsilon} \qquad \textit{Equation 1}$$

$$v = \frac{BV \cdot GF \cdot \varepsilon}{2} \qquad \textit{Equation 2}$$

The material used for the strain gauge is specific due to the thermal expansion that occurs during testing. The alloys have been designed so that the thermal expansion of the material cancels out by the resistance decrease due to the extra heating. Figure 2.8 shows the tool used to measure the resistivity from the strain gauge. First the strain is calibrated before the sectioning is performed and will generate the first strain value ε1. After sectioning a new strain is measured ε2 and the difference is calculated as ε1-ε2. The Δε is used in Hooke's law and with a Young's modulus of 130 GPa in compressive and 120 GPa in tensile will give the stress through the lattice.

Figure 2. The tool used to measure the strain generated from the Wheatstone bridge to measure resistance in a strain gauge. Following is an example of how the stress is calculated from measurements:

First measure the strain ε1 from calibration of the Wheatstone bridge, e.g. 49750. After sectioning, the strain has to be measured once again; ε2 is given, e.g. 50000. This gives the total strain of sectioning (ε1-ε2 = -250), by apply the Hooke's law in compression stress (E=130 GPa) the resulting stress is E*ε= 130 GPa × -250 = -32,5 MPa.

THERMOCOUPLE

Thermocouples will be used to measure the temperature of the stress lattices in the practical experiments. The principle behind it is simple and it can measure temperature accurately enough to fulfill the demands of the testing. By joining two rods of different alloys with one another through soldering at one end and let the two pieces experience a heat change, a difference in voltage will be generated at the soldered point. The voltage generated from this type of action is called the Seebeck effect. This effect is measured in emk (electro-motive force, in this case it is referred to termo-emk because the difference in voltage is generated due to the temperature difference) and is the sum of change of potential in a circuit. On the opposite side of the rods, the non-soldered part is then attached to

a device measuring the change of voltage over the two metals and display the temperature.

INVESTIGATEDMATERIALS

The experimental part will be performed and compared between three materials; Grey iron GJL-250, Grey iron VIG-275/190 and Ductile iron EN-GJS-500-7. It should be noted that the chemical composition is just for reference. Each foundry adjusts their cast iron composition to achieve the mechanical properties demanded of the iron.

1. Ductile Iron En-Gjs-500-7
2. Grey iron, VIG 275/190
3. Grey iron, GJL-250
4. Grey Iron, VIG 275/190

Two foundries produced the stress lattices used for the experimental part, Skovde foundry and SKF's foundry.

The mechanical requirements are as follow:

- Tensile strength is minimum 275 MPa
- Minimum hardness of 190 HB
- No specification regarding elongation and yield strength
  (VISG 275/190 SR, STD 310-0001 [Volvo standard])

IV. THE PRACTICAL HEAT TREATMENTS

Table 1. The specified chemical composition of VIG-275/190 and the measured

Che	C	Si	Mn	P	S	Cr	Ni	Mo	Cu	Sn	Ceqvi.
AC/SR	3,05-3,25	1,7-2,0	0,5–0,8	max 0,08	0,08–0,14	0,1–0,18	-	0,2–0,3	0,8–1	0,04–0,07	3,65–3,94
Lattice	3,32	1,99	0,56	0,03	0,08	0,11	0,04	0,22	0,91	0,033	3,83

Table 2. Chemical composition of the GJL-250 cast iron. Ti and Sn are trace elements and are not part of the alloy.

Chemical composition	C	Si	Mn	P	S	Cr	Ni	Mo	Cu	Ti	Sn	Ceqvi.
AC/SR	3,1–3,4	1,8–2,3	0,6–0,8	Max 0,2	0,06–0,12	-	-	-	-	-	-	3,6–3,9
Nr. 1	3,41	1,84	0,7	0,021	0,071	0,052	0,041	0,012	0,284	0,007	0,005	3,88
Nr. 2	3,4	1,88	0,74	0,019	0,08	0,045	0,042	0,011	0,299	0,007	0,005	3,88

Table 3. The specified chemical composition of GJS 500-7

	C	Si	Mn	P	S	Cu	Mg	Ni	Mo
As cast/SR	3,2-4,0	1,5-2,8	0,05-1,0	0,08	0,02	0–0,5	0,03–0,08	-	-
Lattice	3,49	2,54	0,3	0,028	0,007	0,33	0,039	0,03	≤0,01
Lattice SKF	3,49	2,32	0,42	0,016	0,009	0,30	0,044	0,02	≤0,01

Table 4. The heat treatment cycles of the first seven heat treatments for VIG- 275/190:

Trial	Heating rate	Hold time	Cooling rate	Drop temperat
1	67	2,5	75	200
2	**200**	2,5	75	200
3	200	**0**	75	200
4	200	**5**	75	200
5	200	2,5	**150**	200
6	200	2,5	75	**420**

Table 5. The four reamining heat treatments of VIG 275/190:

Trial	Heating rate	Hold time	Cooling rate	Drop temperatu
7	250	0	150	200
8	200	2,5	75	200
9	67	2,5	150	300
10	67	5	75	100

Table 6. The remaining heat treatments of GJL-250

Trial	Heating rate	Hold time [h]	Cooling rate	Drop temperat
7	200	**1h 15min**	75	200
8	200	2,5	-	600
9	200	2,5	**350**	200

Table 7. The reduced heat treatment plan for Ductile Iron GJS 500-7:

Attempt	Heating rate	Hold time	Cooling rate	Drop temperat
2	200	2,5	75	200
3	200	0	75	200
4	200	**5**	75	200
5	200	2,5	**150**	200
6	200	2,5	75	**420**
7	200	2,5 @ 540 °C	75	200

Table 8. The simulated residual stresses after heat treatment from drawing.

Simulation:	Tensile stress point 1	Tensile stress point 2	Compressive stress point 3 [MPa]
From drawing (v7)	10,8	5,3	-23,1
Low hold time (v17)	12,6	4,65	-19,9
High cooling rate	12,3	4,7	-19,3
No hold time + high cooling rate	18,2	9,7	-33,5

Table 9. Remaining residual stresses after simulated heat treatments of Skovd:

Simulation:	Tensile stress point 1 [MPa]	Tensile stress point 2 [MPa]	Compressive stress [MPa]
As cast	46,4	36,8	107,3
In use HT (v2)	12,6	4,9	19,9
No hold time (v3)	16,3	6,7	25,9
Inc. cooling rate (v6) - 110	15,4	7,4	26,8
Inc. cooling rate (v5) - 150	15,7	7,6	27
Increased quenching temp. (v8) - 200	15,1	7,1	26
Increased quenching temp. (v9) - 300	15,2	7	26
Hold time 2.5h (v13)	11,9	4,3	18,9
Increased cooling rate and quenching temp.	12,3	4,6	19,2
Extreme values (v15)	12,2	4,6	19,2
Hold time 1h (v16)	13,8	5,4	21,3

Table 10. The simulated residual stresses after heat treatment for ductile iron GJS-500-7.*If no version number is provided a previous version has been modified

Simulation:	Tensile stress point 1	Tensile stress point 2	Compressive stress point 3 [MPa]
After Solidification	69,8	61,2	174,9
From drawing (v23)	20,9	14,6	43,2
No hold time (v24)	31,2	24,2	67,9
Low heating rate	20,6	14,3	42,4
5h Holding time (v26)	15,7	9,7	30,9
150 °C/h Cooling (v27)	19,9	13,6	40,7
420 °C drop temp.	19,3	13,1	39,3
GJS-600-3	76,2	66,3	191,1

V. RESULT AND DISCUSION

The results from simulations and practical experiments are presented and explained in this chapter.

SIMULATION

The first simulation is performed to calculate the residual stress after the solidification and cooling. Thereafter simulation of heat treatment parameters are performed with varying parameters such as heating rate, hold time and cooling rate. Magma5 simulates residual stresses over time in the casting process and the relieving of heat treatment. The first simulation includes the in gate system; by simulate the solidification process and removing the in gate system the residual stresses gets slightly higher, but no significant difference. The residual stresses after casting will be the output values compared to the stress after heat treatment. Figure 3 shows the residual stresses in X-direction after solidification. Three points are chosen to show the local stress values. First point is placed inside the middle section 12.5mm down. Second point is on the surface of the middle section and the last point is placed on the surface of the compressive section.

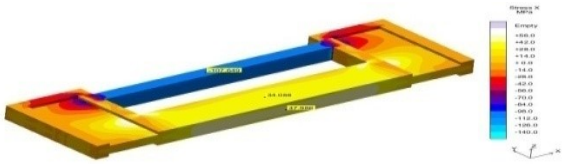

Figure 3. Simulated solidification process of stress lattice (simulation v1).

In Figure 4. seen below is the lattice after the heat treatment. The simulation shows that the tensile stresses in point 1 and 2 have been reduced by 84% and 77% respectively and compressive stress reduced by approximately 78 %.

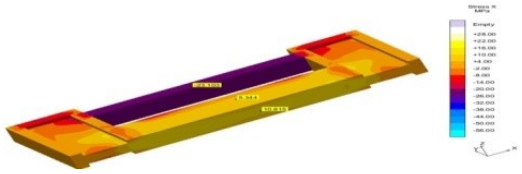

Figure 4. Simulation result of the residual stresses after heat treatment (simulation v02).

To confirm the relieving effect of the sectioning method a simulation is performed with the same scenario. The stress revlieving section cut can be simulated as a machining operation after heat treatment. Figure 5 shows the stress after heat treatment to the left and remaining stress after sectioning to the right. As shown almost all stress is relieved in the compressive section, in the tensile section the residual stress is relieved and causing compressive load due to deformation after cutting. Along the edge of the thick section increased compressive stress are seen.

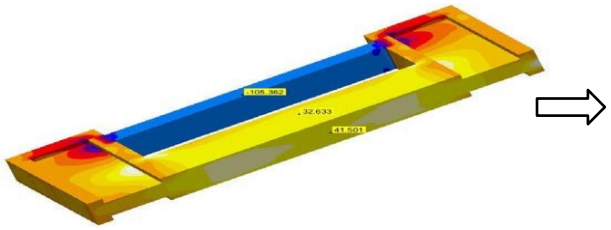

Figure 5. Simulation of the stress relieving section cut.

Simulations of GJL 275/190 and GJL-250

Simulations of both GJL 275/190 and GJL-250 are the same in Magma5 and there are no differences between the two materials during simulations. Therefore they share the same results and are bundled together. To find when the most stress is relieved the time, stress and temperature is plotted for each run. In figure 6.4 the stress relieving process is showcased and the most stresses have been released by the time the temperature is at its peak. Meaning the majority of the stress relief has already occurred before phase 2 has started.

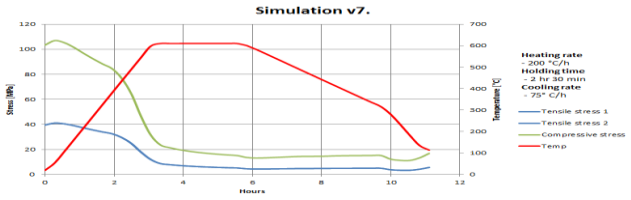

Figure 6. Simulation v7 of stress relieving over time. The red curve shows the temperature over time which is followed by the stress relieving effect.

Figure 7. shows the stress relieving effect when the hold time is shortened from 2.5 h to 1h 15min. Both the tensile and compressive stresses have changed but only slightly compared to v7 in figure 6

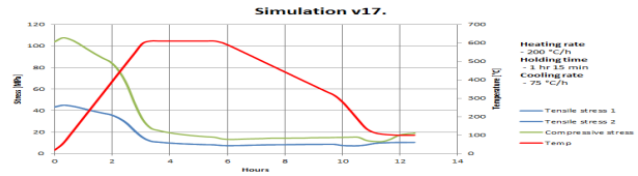

Figure 7. Simulation v17, from drawing with 1h 15min h hold time. Tensile stress 1 & 2 are the same.

Figure 8 shows the stress relieving when the cooling rate is increased from 75 °C/h to 150 °C/h. No major difference of the residual stresses can be observed by increasing the cooling rate from the simulation program. A concern regarding the later versions of the simulation is the dip in stress at the 8:30 mark. This is thought to be an accumulated error and gets progressively worse. It is possible that the change in cooling rate is the cause of the dip due to different values and more extreme parameters cause a larger change in curve.

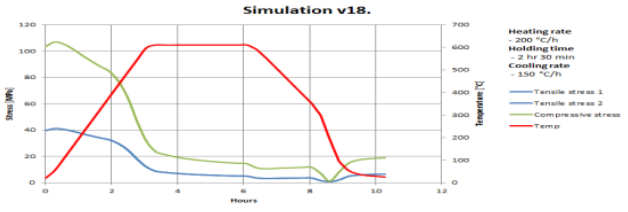

Figure 8. Simulation v18, drawing with a faster cooling phase of 150 °C/h.

Table 8 shows the remaining residual stresses after the simulated heat treatments, no major effect is obtained by either of the hold time or cooling rate separately.

Combining the two parameters seems to have a synergetic effect and increases the residual stresses in both tensile and compression with an estimated 40% compared to each of the parameters alone.

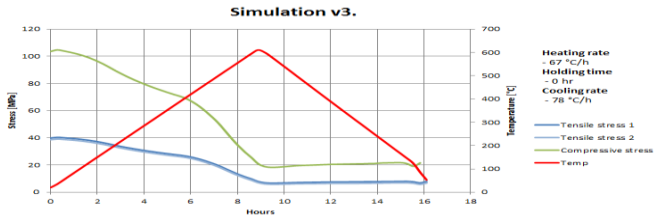

Figure 9. Heat treatment without holding time (simulation v3).

The different simulations have been put into separate tables to be more easily observed. The influence of drop temperature presented in Figure 10. There is not much difference between each simulation. All three simulations have a residual stress of 25 MPa in compressive and 15 MPa in tensile stress. The recommendations given by the Skövde drawing seems to be correct.

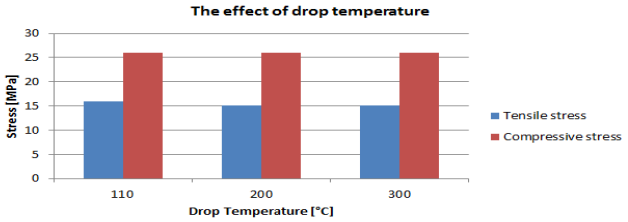

Figure 10. The residual stresses with changed drop temperature from simulations.

The significance of holding time is shown in Figure 11 and it follows a decreasing exponential curve. The variance between each simulation is large and there is a clear indication that holding time has an effect on the residual stresses. Looking at the curves presented to the right in table 6.3 there is a noticeable difference between the relaxation of compressive and tensile stresses. Compressive stresses are lowered for each run while the tensile stress remains the same in both 2.5h and 5h runs.

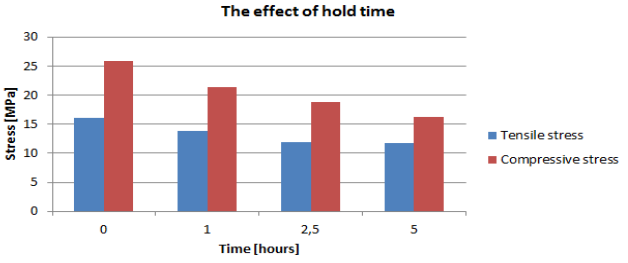

Figure 11: The variation of residual stresses due to changed holding time.

Reaching the last parameter that can be changed is the cooling rate. From the Figure 12 seen below there is no difference between the different cooling rates. Neither compressive nor tensile stresses changes between the three runs and the resulting residual stresses are kept at the same levels.

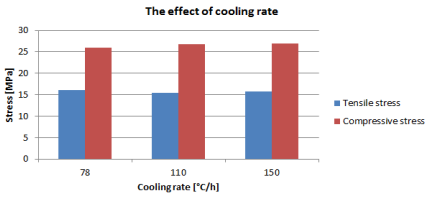

Figure 12: The influence of cooling rate on residual stresses.

Based on previous runs an optimal heat treatment curve was created in order to test the combination of all parameters. The optimized curve can be seen in Figure 13. A heating rate of 67 °C/h was chosen since no other option was possible. Phase 2 consists of a holding time of 5 hours at 610 °C. Lastly, phase 3 has a rapid cooling of 300 °C/h with a drop temperature at 300 °C. This makes the cooling phase less than 2 hours long. This is impossibility in the practical case and would create new residual stresses.

The optimized heat treatment seems to reduce most residual stresses and neither compressive nor tensile stresses are above 20 MPa. By looking at the curve many bumps can be observed with an especially big one at the end. This bump is visible in other simulations as well but it is very predominant in this version. The irregularities seem to occur when the temperature changes and might be an artifact due to the way Magma handle transitions between different phases.

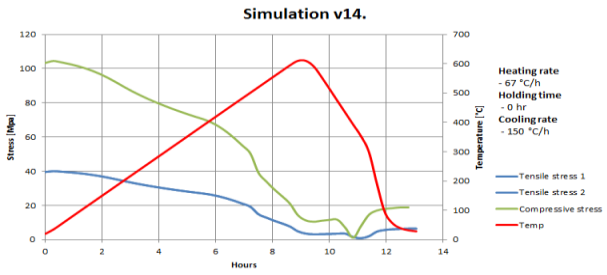

Figure 13: Heat treatment parameters based on the optimal result (Simulation v14).

A summarization of all heat treatment simulations is compiled in table 6.2. Each simulation was done in the same way seen in Figure 7.7 but with one parameter

changed. This was done to observe and analyze the effect of each parameter. In general Magma 5 seems to have difficulties handling a rapid cooling rate and seem to disregard any extreme parameters; the results seem to be the same regardless. The assumption is that the simulated results are not equal to a physical scenario and therefore the results from the simulation might not correlate with the practical testing.

By comparing the simulations of Skövde foundry HT and the varying parameters the simulation gives a prediction of what will affect the relieving of residual stresses. But the results also indicate that the cooling rate and quenching temperature will not affect the remaining residual stresses. This gives suspicions of what the program can simulate and what the limits are. The cooling rate varies from 78 °C/h to 150 °C/h, and does only have a minimal impact on the residual stresses. Whether or not this is accurate can't be said and practical testing is necessary in order to confirm or disapprove it

1) Simulating ductile iron GJS-500-7

The ductile iron is simulated with the same parameters as simulation v7. After the solidification, residual stress is much higher compared to the grey iron and this is due to the higher mechanical properties of the ductile iron. The stress after solidification is shown in Figure 111.

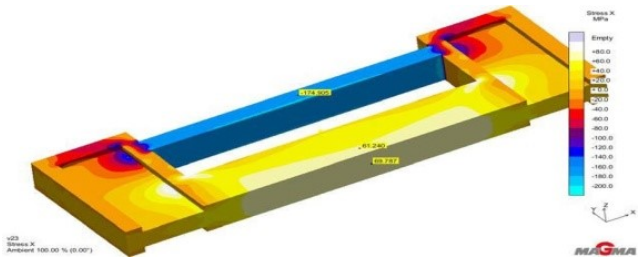

Figure 14: The simulated residual stresses after solidification of ductile iron GJS-500-7.

In table 10 the stresses of both tensile and compressive points are presented. The table shows that the hold time has a significant effect and that a higher cooling rate will not be affect the stress generated. The stronger ductile iron grade GJS-600-3 was also simulated in order to confirm that a higher tensile strength generate higher residual stresses in Magma5. This would explain why the stress is higher in GJS-500-7 compared to the other two cast irons tested.

2) VERIFICATION OF SIMULATION MODEL

By comparing the practical testing and simulations it can be seen that the simulations tend to have higher residual stresses compared to the reference lattices tested. In the figure below there is a clear difference in cooling rate between the real material and the simulated one. Another observation is that the phase transformation that occurs at ~720 °C, from austenite to pearlite, is non-existent in the simulation. When this transformation occurs in the physical material it generates heat and slows down the overall cooling rate of the material. Due to the absence of the transformation in the simulation no such reduction of the cooling rate exists. Therefore the cooling is much more rapid, creating a shift in the plot, generating a bigger discrepancy between the experimental and simulated case, especially after 730 °C. In the simulation this rapid cooling is reflected in the residual stresses, yielding values higher than the physical material, Figure 15.

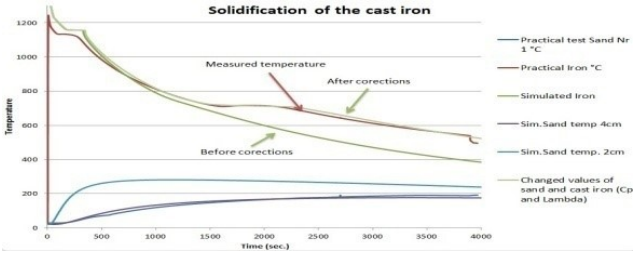

Figure 15. Calibration of the simulated solidification process of GJL-250.

In an attempt to make the simulation and the physical solidification process as similar as possible changes were done to material parameters in the Magma database. By changing the heat diffusion and thermal capacity of both the moulding sand and the iron the overall residual stresses were reduced in the simulation. The reduction was small and the improvements didn't make any major changes to the resulting stresses calculated by Magma5. The reduction was a total 9 MPa in compressive lowering the stress to 98 MPa.

The stresses in tensile mode did not change more than 2 MPa in the simulation with previous mentioned improvements. All of the values from the simulation before and after can be seen in Figure 16 below.

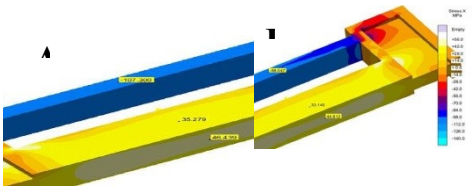

Figure 16. In the figure to the left (A) is the simulation before the changes to the material parameters and to the right (B) are the updated parameters with a lower stress.

RESIDUAL STRESS MEASUREMENT

This chapter shows all the resulting measurements of residual stresses. The changed parameters and resulting stress values will be compared to each other to find the most optimal heat treatment and the valuation of each change.

The residual stress is measured after solidification to get the reference stress for each material. These stresses will be used as a baseline before the heat treatments. The Figure 17 shows how the measured stress between the materials. It's clear that the residual stress after solidification varies to the materials strength.

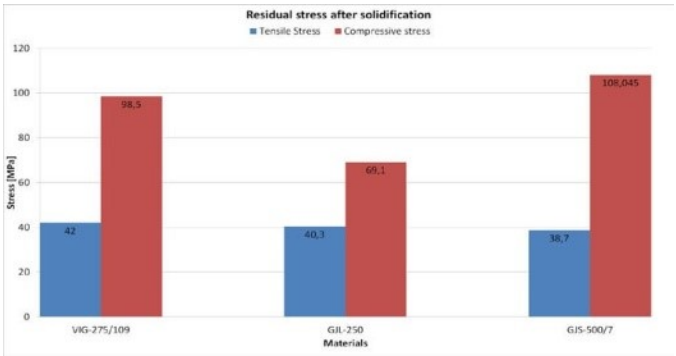

Figure 17. The reference residual stress as cast for each investigated material.

3D SCANNING THE COMPONENT

To investigate a possible bending load case in the stress lattice the geometry was scanned before and after sectioning to see how the deformation took place. The scanning was performed on stress lattice R3 and R4 (Reference 3 and Reference 4, two as-cast lattices) and resulting strain is shown in Figure 6.18. The significant deformation is along the X-axis, as desired. In R4 this is the case, less than 10% has been deformed along the Z-axis (Bending direction) and is therefore not presented in Figure 7.13. However, in R3 this is not the case; any deformation along the X-axis is less than that of R4's values and there is an equal amount of deformation along the Z-axis in the other half of the lattice. Analyzing both of these cases raise the question if some other lattices have deformed the same way as R3.

Regarding the bending and the presumed effect it might have on the overall stress results some calculations have been made, assuming an exaggerated dislocation along the Z-axis of 0.1mm, ten times the value seen in R3. With this exaggeration a difference of 40% could be created between the top and bottom side of the lattice. From this the conclusion is that these results show that the bending seen in the lattices is not causing the large irregularities of stress values measured. Using strain gauges on both sides and taking the average of the two values eliminates this error as well.

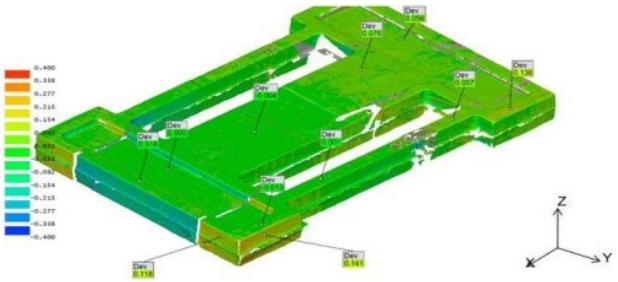

Figure 18. Shows the scanning of lattice R3. Deviation after sectioning is measured in mm. The marked points on the surface indicate the deformation. The deviation is significantly larger in x-direction, but the bending case in y-direction can't be ignored.

Cast iron VIG 275/190

Find the resulting temperature vs. time plots of each HT trial see appendix (Heat treatments). All parameters for heat treated lattices are introduced in the method chapter. Following will describe the result and variation between the heat treatment runs. Resulting stresses are presented from the experiments in this chapter, both from the sectioning and the result of the different heat treatments performed. The stress results are presented in table 11.

Table 11: The resulting stress values are calculated to compensate for the bending load case in both compressive and tensile sections. *Values from HT-SL did not correspond with the stress case and are therefore omitted.

Lattice	Average Compressive MPa	Average Tensile MPa
R1 (No heat treatment)	*110*	*37*
R2 (No heat treatment)	*90*	*53*
R3 (No heat treatment)	*93*	*37*
R4 (No heat treatment)	*101*	*41*
Average Reference stress	***98,5***	***42***
HT-SL (Skövde heat treatment large oven)	*Removed**	*Removed**
HT-SS (Skövde heat treatment small oven)	*12*	*14*
HT-1 (heating 67 °C/h)	*27*	*9,6*
HT-2 (heating 200°C/h)	*33,3*	*3,6*
HT-3 (no hold phase)	*34*	*13*
HT-4 (5h hold phase)	*24*	*9,3*
HT-5 (150 °C/h cooling rate)	*29,2*	*11,9*
HT-6 (400 °C drop temperature)	*10,9*	*30,8*
HT-7 (no hold time and 150 °C/h cooling rate)	*49,7*	*17,1*
HT-8 (redo the HT-2)	*31,3*	*10,9*
HT-9 (time efficient HT of Skövde)	*31,3*	*10,9*
HT-10 (The HT- of Skövde)	*17,6*	*6,4*

The Figure 19 shows the remaining residual stress after heat treatment. As shown varying heating rate between 67-200 °C/h has a significant effect on the remaining stress. The hold time at 610 °C also have a significant effect on the residual stress. Cooling rate and drop temperature, however, not showing any larger effect on the stress results. By combining high heating- and cooling rates and no hold time the stresses are much higher which is proven with the last treatment (HT-7).

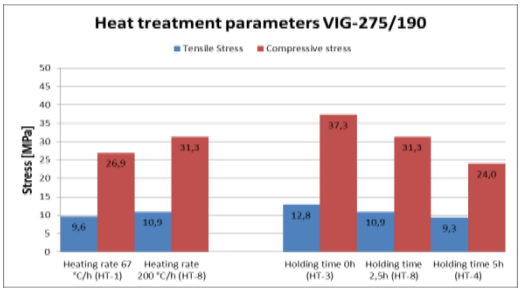

Figure 19: Heat treatment parameters effect on residual stresses.

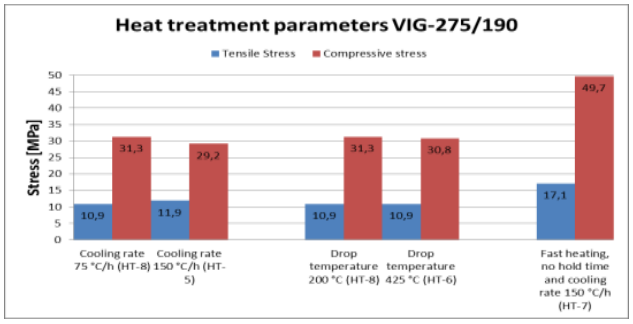

Figure 20. The effect of changing cooling rate and drop temperature on VIG-275/190.

At last the current used heat treatment cycle in Skövde is compared to what is evaluated as a time saving heat treatment cycle based on result from previous changed parameters. As shown, the heat treatment used today at Skövde foundry obtains much lower residual stress. This is mostly an effect of combination of parameters. The previous heat treatments only change one parameter each run and will therefore not obtain as high relieving effect as Skövde HT, Figure 21.

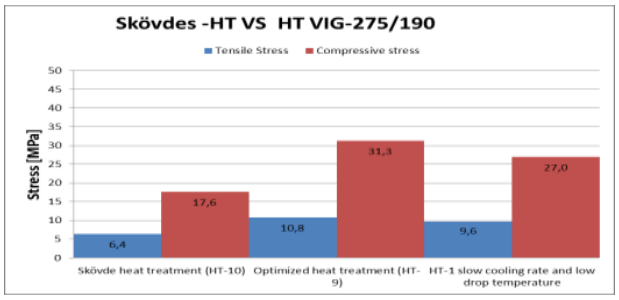

Figure 21. Stresses measured from the suggested rapid HT and the current HT in Skövde foundry.

The previous table shows the effect of hold time which highlights the importance for the material to spend time at high temperature. From the HT plots (Appendix B) the time spent above 500 °C is calculated and plotted against the stress relief. The plot only considers the time spent over 500 °C regardless of rapid heating, cooling rate and drop temperature since this indicates to be the most important factor of stress relieving. From the plot a second order relationship exists between relived stress and time spent above 500 °C. The assumption is that the curve will flatten out close to 10 hours, shown in Figure 22.

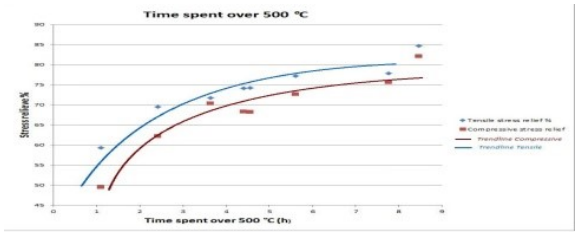

Figure 22. Stress relieve in % compared to the time spent over 500 °C.

3) **Cast iron GJL-250**

The unalloyed cast iron, GJL-250 responded well to the heat treatment and all tested parameters had an effect on the resulting residual stresses. Holding time was still the most influential parameter in the VIG 275/190. The trend of the holding time is seen clearly in table Figure 23. Increased cooling rate and drop temperature seemed to increase the residual stress level, something not observed in VIG 275/190.

Having no hold time with cooling rate and drop temperature according to the test plan provides a significant reduction in residual stresses compared to the reference. With only 75 minutes holding time the residual stresses are halved relative to the heat treatment with no holding time. Compared to the reference lattice with no heat treatment the stresses had been reduced with ~75%. Due to having only 9 lattices to use for the experiments no synergy effects were investigated and all tests have only had one varying parameter.

HT-8 was the last heat treatment performed and was done to investigate the buildup of residual stresses and to provide insight in the casting process. The temperature of the lattice, at 610 °C is close to the same temperature as the cast iron has when the mould is broken up and separated from the goods.

Heating rate was not investigated in GJL-250 due to limited amount of stresslattices. Furthermore, investigating heating rate was only done to VIG-275/190 in order to provide information regarding Skövde Foundry's own heat treatment.

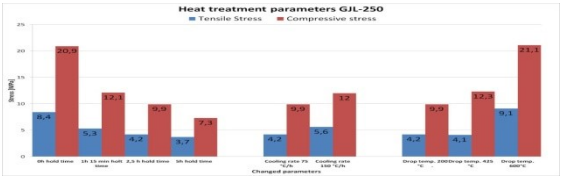

Figure 23. The residual stress after HT of GJL-250.

When all HT are performed they are summarized in Figure 24 the trend shown by VIG 275/190 is not as clear for GJL-250. Residual stresses are more easily removed in the un- alloyed material and parameters such as cooling rate and drop temperature also seems to have affected the resulting stresses. The scatter is more apparent but still a trend shows that the time over 500 °C is important.

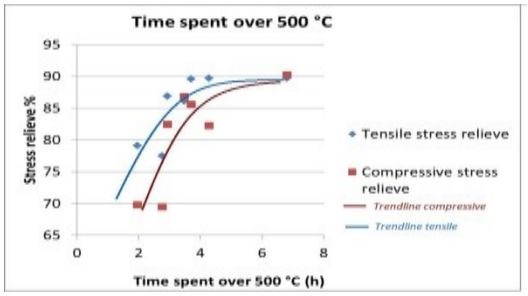

Figure 24. The stress relieve vs. time spent over 500 °C, GJL-250. Cast iron GJS-500-7

With four lattices available for heat treatment some adjustments were made in order to fully focus on the most important parameters. HT-2 is the heat treatment described in the plan and will provide a reference value that can be compared with the grey irons. The other heat treatments (HT-4, HT-5, and HT-6) had the same profiles as for the grey irons.

Seen in Figure 25 is the stress after each HT. HT-4 seemed to respond well to the increased hold time and showed low stress. Comparing HT-2 with HT-5 and HT-6 shows no remarkable difference of changed parameters in the cooling phase. The differences are roughly within 2 MPa in compressive stress and less than 2 MPa in tensile stress. The increased stress by higher cooling rate indicates to some effect of increasing the cooling rate above 400 °C. In short it looks like the GJS-500-7 has a tendency for faster creeping and responds quickly to the HT.

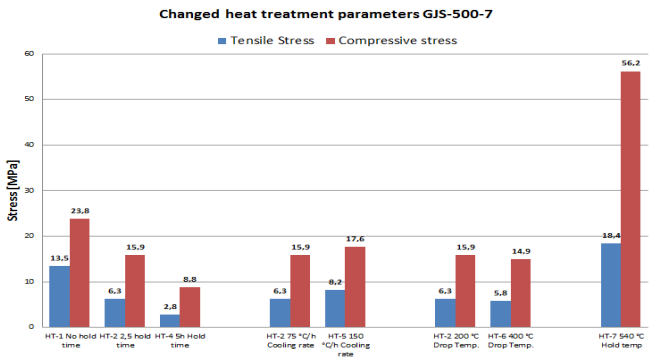

Figure 25. The residual stress after heat treatments conducted on GJS-500-7

Comparing the results with simulations shows once more that Magma5's model of GJS-500-7 is not fully correct. The values provided from the simulations were far above the actual stress with values more than twice the amount of stress. The stress values from the simulations have been presented in table 10. Still the simulations predicted the effect of the different parameters correctly and HT-2, HT-5, and HT-6 had similar values in the simulation, just as the measured values seen in the table above. Yet again do the tests confirm the importance of holding time and the residual stresses are reduced significantly with a longer holding time. From HT-7 where the holding temperature was reduced from 610 °C to 540 °C confirms that that reducing the holding temperature can severely affect the residual stresses. Comparing HT-1 and HT-7 shows the difference between having a higher temperature or longer holding time.

COMPARISON OF THE MATERIALS

In Figure 26 all investigated cast iron alloys are presented with the stresses as cast and after HT-2, which is the recommended heat treatment from Volvo. From the table there is a clear difference seen between the alloys not using Mo and Cr. Both the unalloyed cast iron, GJL- 250 and the ductile iron GJS-500-7 have roughly 14% of the stress before HT, while in VIG 275/190 the difference is 33/25% in compressive and tensile respectively. The difference seen in relaxation between tensile and compressive in all the alloys is due to the variation in cross section area and volume. This is especially noticeable in the case of VIG 275/190. Another value to note is a low compressive stress in the GJL-250 reference and this low value is assumed to be due to an errant strain gauge, without that value the stress is 76 MPa. This assumption is because the simulation has shown reliable values regarding the GJL-250 cast iron.

Furthermore, the HT-2 has proven to be successful for the two cast irons not containing Mo or Cr and most of the residual stresses has been relived during the process. With regards to VIG- 275/190 a 2 hour and 30 min hold time is not enough to fully reduce the stress.

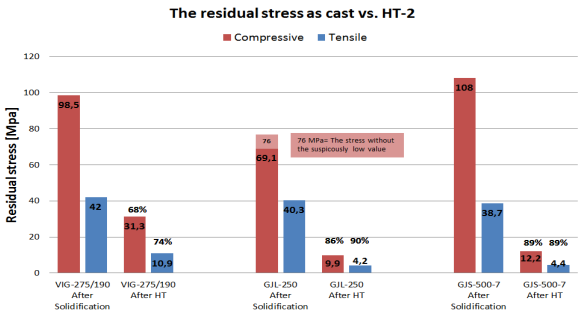

Figure 26. A comparison of residual before and after HT-2. The % values show the residual stress reduction during HT.

In Figure 27 the simulations of casting process and heat treatment (drawings) are compared to the practical testing. For the VIG-275/190 simulations predict higher stress after solidification and lower stress after heat treatment, i.e. a higher relieving effect. In the ductile iron GJS-500-7 the simulations also predict a higher stress after solidification but also higher stress after heat treatment.

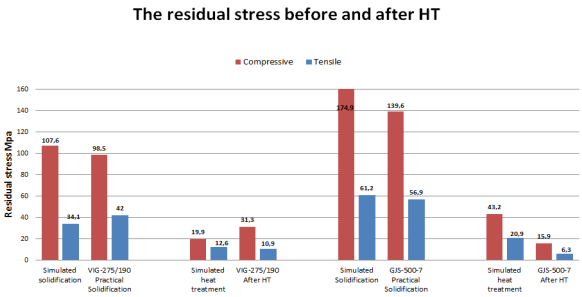

Figure27. Comparison of simulations and experimental test on residual stresses. GJL-250 is not included since it uses the same simulation data as VIG-275/190.

EXPERIMENTAL VERIFICATION OF MATERIALS

The verification of the three materials analyzed is done in order to confirm the composition of the material, the microstructure, hardness and the distribution of the ferritic and pearlitic matrixes. Stresses presented previously are valid for the type of materials presented in this chapter.

4) Grey iron, VIG-275/190

The hardness test shows that the hardness differs between the tensile and compressive sections. The assumption is that the cooling in these sections is different, with a higher cooling rate in the compressive section increasing the hardness. The increased cooling rate changes the microstructure towards smaller graphite and finer pearlite that will provide a higher hardness. The conclusions of hardness tests are the values are within expectations and exceed the specified minimum requirement, table 6.12. In the compressive section of the GJL- 250 the hardness differentiates a lot from the tensile section. Regarding the ductile iron, GJS- 500-7 the hardness value is high and some values are above the specification. The same hardness values were seen in both SKF and Skövdes lattices and hardness values this high indicates incorrect distribution of pearlite and ferrite, caused by larger undercooling.

Table 6.5, Hardness measurement (Brinell 2,5mm with 187,5kg). Each value is a mean value of three indentations.

Hardnes	VIG-	Grey iron,	GJS-500-7	GJS-500-7
Compress	*258*	*228*	*240*	*247*
Tensile	*231*	*185*	*231*	*218*
STD	*min 190*	*190-240*	*170-230*	*170-230*

The amount of graphite in VIG-275/190 is varying between the tensile and compressive section. The tensile section obtains a graphite amount of 11,4% and the compressive is 8,8% the differences in amount of graphite is influenced by the polishing of the micro samples. Graphites loosely fixated and are very easily removed during the grinding process, thus potentially creating this error. The tests were performed on the reference lattice, R1. No visible difference can be seen between the two samples; the graphite structure looks similar for both images and has a formation of the graphite is I accordance to *EN ISO 945-1:2008.* The type of flakes is the most similar to A + E structure.

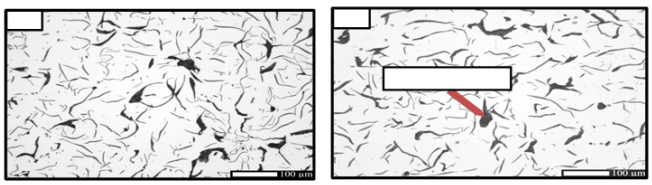

Figure 28. The microstructure of graphite VIG-275/190. a) The compressive section b) The tensile section.

Tensile test is performed to confirm that strength is according to specification. As shown in Figure 18 the lattice is cut in 6 tensile samples and sent to be manufactured as tensile specimens. Three specimens from the compressive section and three from the tensile section are cut out. The test bars are of type 7C35.

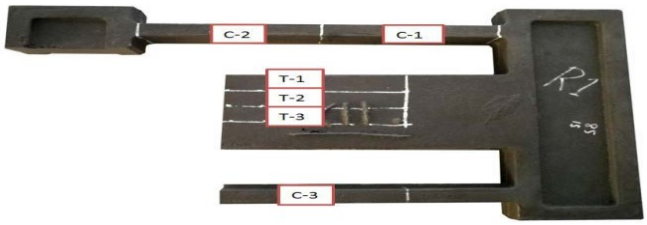

Figure 30. The location of where the tensile test specimens are cut out.

All components were not fully functioning in the testing machine when the tensile testing started and therefore C-1 and C-2 are not properly set up (missing values from extensometer). C-3 had its fracture outside of the extensometer gauge and broke very close to its attachment but the result seems to fall within the expected value.

All six tested bars fulfill the requirements of at least 275 MPa (Rm). The compressive bars show a higher tensile strength and this is due to the higher cooling rates in those sections of the lattice. The microstructure is finer and therefore the strength is higher given by the Hall-Petch relation. T-2 had low values compared to the other tensile bars and a graphite pore is in the crack zone which would explain the low value, shown in Figure 19. The testing was conducted by the standard EN ISO 6892-1 A222.

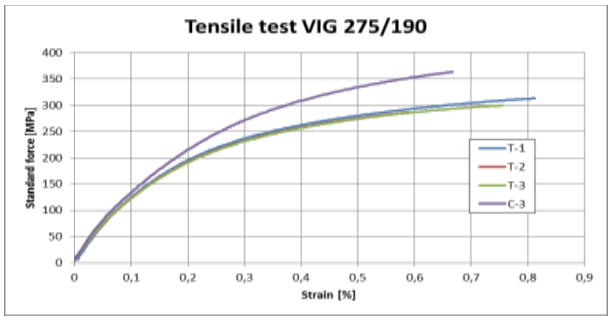

Figure 31. Tensile tests C-1 and C-2 were ignored due to invalid values and T-2 is behind T-1 and T-3.

5) **Grey iron, GJL-250**

In the microstructure samples from GJL-250 the compressive section shows a less distributed graphite structure, 20. The graphite in figure (a) is all type-A shaped, the wanted shape in grey cast iron,. In the thinner part section the graphite shape is changed to B-type graphite due to the under cooling experienced in the section. There is also the transition shape graphite type-D present as well with some smaller portion of type A graphite. It has been stated previously that the hardness of the compressive section is 40 HB higher than the tensile section which would indicate that the microstructure is different and material properties might vary between the thinner and thicker sections.

A brief overview of GJL-250 is given from the two tensile bars tested. Both tensile bars are within the specifications with T-1 being on the verge of 250 MPa tensile strength.

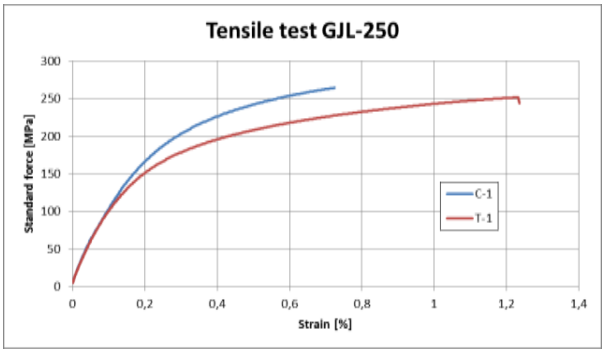

Figure 32. Tensile test of GJL-250. Red curve is the tensile and blue is the compressive section.

6) **Ductile Iron GJS-500-7**

Micro-samples are manufactured to investigate the nodule structure and measure the nodularity and nodule count. There are clear differences in nodule sizes and this is due to the cooling rate being higher in the thinner, compressive section.

The tensile tests of GJS-500-7 show that both bars are outside of the specifications. This is explained by the high amount of pearlite seen in the microstructure. Both the elongation and tensile strength.

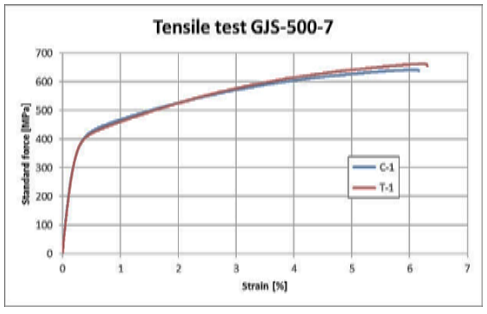

Figure 33. Tensile test of GJS-500-7. Both curves are not within the specifications.

VI. FUTURE WORK

The practical testing had a limited amount of stress lattices. With a higher amount of test lattices a wider range of parameters and their combinations can be examined. Also, an optimized complete heat treatment cycle could be formed for each specific material.

Further investigation of how high temperatures you can reach (hold temperature) without affecting the microstructure and mechanical properties would be interesting to investigate. To reach as high temperature as possible would make creep higher and accelerate the stress relieving. In the pre-study three hold temperatures have been investigated and their respective hardness have been compared. The results indicate that a hold temperature of 650 ° C is too high and changes the mechanical properties of the material,

For the material GJS-500-7 it would be interesting to further investigate how low hold temperature you can reach with same relieving effect to save both energy and time.

VII. REFERENCES

[1]. G. I. Sil'man, V. V. (2003). Effect of Copper on Structure Formation in Cast Iron. In Metal Science and Heat Treatment (pp. 254-258).

[2]. G. Totten, M. H. (2002). Handbook of Residual Stress and Deformation of Steel. ASM International.

[3]. Gjuterihandboken.se. (2015, 01 01). http://www.gjuterihandboken.se/handboken/3-gjutna- material/32-graajaern. Retrieved from Gjuterihandboken: http://www.gjuterihandboken.se/

[4]. Gundlach, R. B. (2005). The effects of alloying elements in the elevated temperature properties of Grey irons. Michigan: AMAX material research center.

[5]. Janowak, J. F., & Gundlach, R. B. (2006). A Modern Approach to Alloying Gray Iron.American Foundry Society.

[6]. Johannesson, B., & Hamberg, K. (1989, 11 24). Spännings/töjnings-egenskaper hos gråjärn avsett för cylinderhuvuden [Internal report LM-54159]. AB Volvo. Technological Development.

[7]. Holtzer, M. G. (2015). Microstructure and Properties of Ductile Iron and Compacted Graphite Iron Castings. Springer.

[8]. Magmasoft. (2017, 01 23). www.magmasoft.com. Retrieved from http://www.magmasoft.com/en/solutions/ironcasting.html: http://www.magmasoft.com/en/solutions/ironcasting.html

[9]. Pentronic. (2017, 04 11). http://www.pentronic.se/. Retrieved from http://www.pentronic.se/start/temperaturgivare/teori-om-givare/tabeller-och- polynom.aspx.

[10]. Schmidt, P. (2016). Cast Iron. Volvo Materials Technology.

[11]. Sn-castiron.nl. (2009). Retrieved from http://www.sn-castiron.nl/en/castiron/en_gjl.html: http://www.sn-castiron.nl/en/castiron/en_gjl.html

[12]. Shaw, M.C. "Principles of Material Removal," Mechanical Behavior of Materials, Vol. 1, 1979, p. 227-253.